Chapter

CO_2 Foam for Enhanced Oil Recovery Applications

Ahmed Farid Ibrahim and Hisham A. Nasr-El-Din

Abstract

CO_2-foam yields improved sweep efficiency in enhanced oil recovery (EOR) applications over that of polymers to avoid potential polymer-induced formation damage. In addition to carbon sequestration in underground formations, CO_2 foam has low water content, which also reduces formation damage in water-sensitive formations and allows for fast cleanup. However, foam stability diminishes in harsh environments such as those with high salinity and temperature and when in contact with crude oil. This chapter highlights the different foam-generation mechanisms and the deterioration effect of crude oil on CO_2-foam stability. More specifically, this chapter investigates using nanoparticles and viscosifiers to improve foam stability. Further, the effects of different nanoparticles, including aluminum oxide, copper oxide, and low-cost nanoparticles such as silicon dioxide, will be demonstrated. Field applications of viscoelastic surfactants and polymers in foam systems are also reviewed. The controlling factor for these different systems is the foam stability and improved oil recovery.

Keywords: CO_2 foam, crude oil effect, foam stability, EOR, nanoparticles, viscoelastic surfactants

1. Introduction

Gas injection has been used widely for enhanced oil recovery (EOR) application. Carbon dioxide (CO_2) gas injection was started for EOR applications in the 1950s to improve oil recovery and provide for carbon sequestration in underground formations [1, 2]. However, CO_2 injection proved impractical at that time due to its low viscosity compared to formation fluids, leading to viscous fingering and early breakthrough [3]. Hence, the sweep efficiency and recovery factor were low [4]. Polymer flooding was introduced to reduce the mobility ratio of the displacing fluid to the displaced fluid [5]. The mobility ratio can be calculated using Eq. (1):

$$M = \frac{\lambda_{displacing}}{\lambda_{displaced}} = \frac{(k_e/\mu)_{displacing}}{(k_e/\mu)_{displaced}}, \quad (1)$$

where M is the mobility ratio of the displacing fluid to the displaced fluid, λ is the fluid mobility, k_e is the effective fluid permeability, and μ is the fluid viscosity. Using polymer flooding increases the displacing fluid viscosity. As a result, the mobility ratio decreases, and the viscous fingering is reduced. Hence, sweep efficiency improved, as shown in **Figure 1**. However, polymer flooding is associated with formation damage due to physical adsorption of the high-molecular-weight

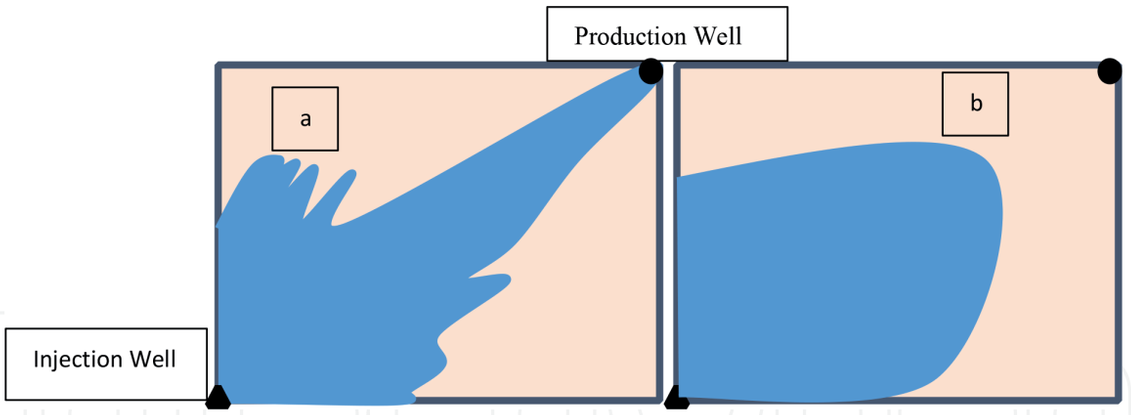

Figure 1.
Areal sweep efficiency, (a) low sweep efficiency and early breakthrough due to viscous fingering at unfavorable mobility ratio values (M < 1) and (b) high sweep efficiency at favorable mobility ratio (M > 1).

polymer on the rock surface and mechanical trapping within the smaller-diameter pore throats [6, 7].

CO_2 foam was introduced in the 1960s as a replacement for polymers to avoid formation damage [8]. Foam has low water content, which reduces formation damage in water-sensitive formations and allows fast cleanup [9]. Foam is a dispersion of a gas (nitrogen, carbon dioxide, or methane) as a non-wetting fluid in a continuous wetting phase. The wetting phase is water that contains surfactant at a particular concentration that is above the critical micelle concentration (CMC). The liquid film separates the gas phase from each other, the outer membranes of the gas bubbles, called *foam lamella*e. The first surfactant families selected for EOR method were petroleum and synthetic aromatic sulfonates [such as alpha-olefin sulfonate (AOS)] because of their availability, lower adsorption on porous rocks, high compatibility with hard water, and good wetting and foaming properties [10, 11].

Bulk foam can be characterized by several properties such as quality, texture, stability, and foam density [12]. Foam quality is the volume percent of gas within foam at a specified pressure and temperature [13]. Foam quality for EOR applications is typically 75–90%. Foam texture is a measure of the average gas bubble size. Foam stability depends on the chemical and physical properties of the surfactant-stabilized water film separating the gas bubbles (lamellae). Foams are metastable systems; accordingly, all foams will eventually break down. Foam stability is measured by the half-life time, which is the time required to lose 50% of the foam volume [14]. In general, as a foam texture becomes finer, the foam will be more stable and will have greater resistance to flow in matrix rock. Foam flow resistance in porous media is measured by the mobility reduction factor (MRF). MRF is defined as the ratio of total mobility of CO_2/brine to foam mobility. When foams become more stable, more resistance to flow is expected and leads to a higher mobility reduction [15].

2. Foam generation

Foam generates in porous media through three different mechanisms: (a) snap-off, (b) lamella division, and (c) leave-behind [16, 17].

In the snap-off mechanism, lamellae are created in gas-filled pore throats as a result of the capillary pressure difference between the pore body and the pore neck [16]. **Figure 2a** shows the foam-generation process by the snap-off mechanism. As

DOI: http://dx.doi.org/10.5772/intechopen.89301

the gas phase displaces the liquid zone, the difference in capillary pressure between the pore body and the pore throat forces the wetting phase (water) to flow back and then snap-off the gas phase.

Lamella division generally occurs when a foam lamella that is larger than that of the pore body approaches a "branching point" and divides into two or more bubbles (**Figure 2b**). If the lamella is at a branching point with more than one path that requires the same pressure for the lamella to flow, the lamella divides into two bubbles or lamellae [18].

Leave-behind occurs when the gas enters a porous medium that is initially saturated with a liquid or when two gas fronts approach a pore space that is filled with liquid; these processes squeeze the liquid into a lamella (**Figure 2c**). The leave-behind mechanism typically forms a weak foam because the generated lamella is parallel to the flow direction [17, 18].

3. Experimental evaluation methods

3.1 Bulk foam stability and microscopic analysis

Foams are generally described in terms of their foamability, which is the ability of a foaming solution (water in the presence of foaming agents) to form a foam. Bulk foam stability or formability tests are static tests that can be used for screening different parameters such as foaming agents, concentrations, salinity, and effect of crude oil [20]. At ambient conditions, foamability of a solution can be studied by performing a shake test [21]. At high-pressure/high-temperature (HP/HT) conditions, foam can be generated by gas sparging into an HP/HT

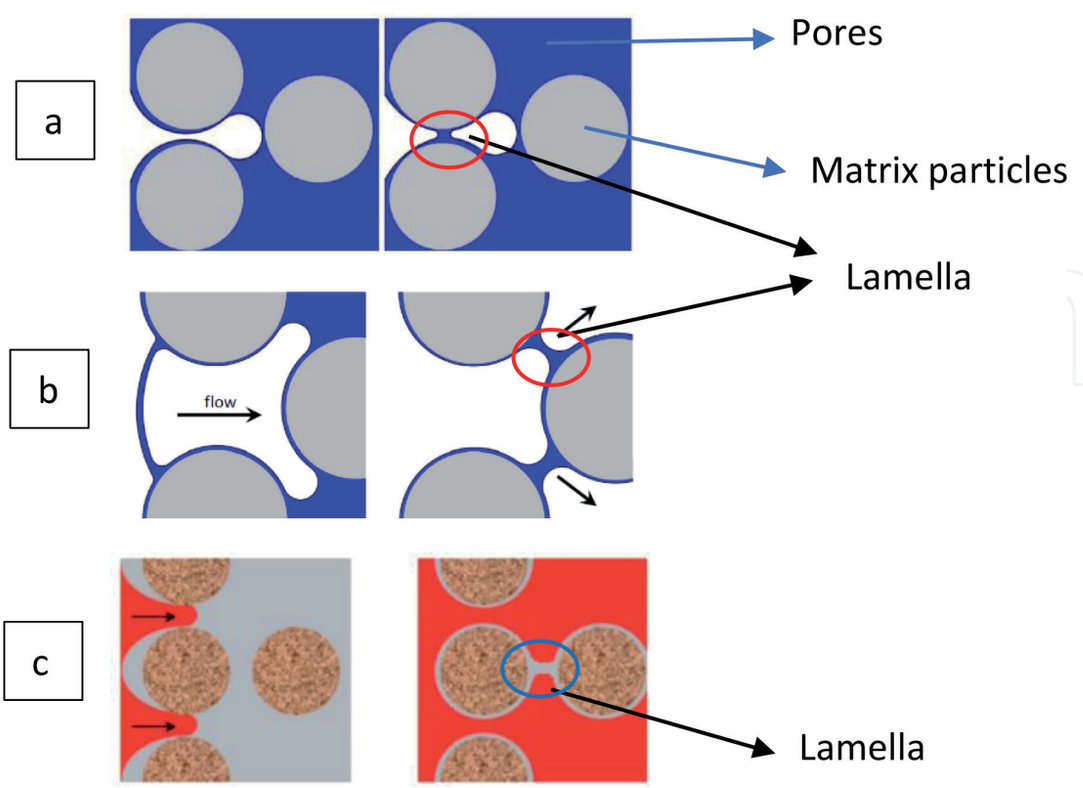

Figure 2.
Foam lamella generation mechanisms: (a) snap-off mechanism, (b) lamella division, and (c) leave-behind (after [19]).

visual graduated cell [22, 23]. The foam half-life time can be measured by monitoring the foam height over time.

Additionally, bubble-scale experiments can be conducted under an optical microscope to investigate the foam stability [24]. The foam bubbles are allowed to stabilize and are then placed on a microscope slide. The foam texture and the thin liquid films (lamellae) are then monitored with time to investigate the foam decay rate [23]. **Figure 3** shows a microscopic image for an AOS foam system in contact with a crude oil.

3.2 Macroscopic sweep experiments

Different flood experiments can be conducted to evaluate the foam performance in porous media. Glass bead packs or cores can be used to represent the porous media. Three distinctly different modes are used for foam injecting: (1) alternative injection of gas and liquid with foaming agents, (2) co-injection of the gas and the liquid phase at the same time, and (3) injection of pregenerated foam. Foam stability usually quantified by the oil recovery and MRF. The MRF can be calculated by comparing the pressure drop across the core during foam injection to the pressure drop after gas injection [15], as described in Eq. 2:

$$MRF = \frac{\mu_f}{\mu_b} = \frac{\left[\frac{kA\Delta p}{QL}\right]_f}{\left[\frac{kA\Delta p}{QL}\right]_b} = \frac{\Delta p_f}{\Delta p_b}, \quad (2)$$

where Q is the total flow rate, k is the absolute core permeability, A is the cross-section area of the core, L is the core length, μ is the viscosity, Δp is the pressure drop across the core, and the subscripts "f" and "b" represent the experiments with and without foam, respectively. The pressure buildup along the porous medium indicates foam-generation and gas mobility reductions [25]. A higher pressure drop signifies viscous foam and considerable resistance to gas mobility in porous media.

Dual coreflood experiments can be conducted to evaluate the divergent ability of foam systems within heterogeneous systems [23]. The foam is injected in two parallel cores with different permeabilities. The stable foam will be generated in the high-permeability formation and divert the flow toward the low-permeability core that improves the sweep efficiency and increases the oil recovery.

Macroscopic sweep experiments are usually combined with X-ray computed tomography (CT) measurements. CT scan analysis can be used to determine the porosity, oil distribution, and foam propagation inside the porous medium.

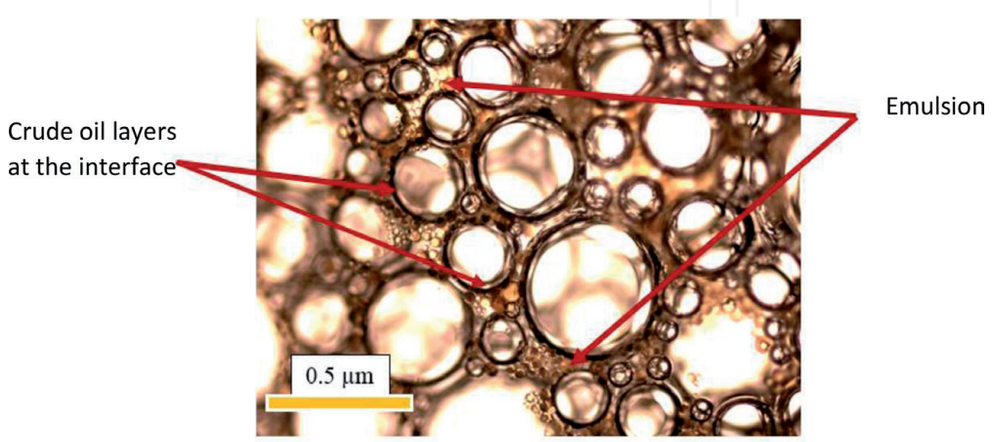

Figure 3.
Microscopic image of AOS foam in contact with a crude oil (5×) [23].

4. Deterioration effect of crude oil

The instability effect of crude oil on the CO_2-foam system is another challenge for the use of this foam in EOR applications [26]. Crude oil composition, especially the presence of light components, decreases foam stability [27]. Foam stability decreases in contact with crude oil as a result of direct surface interactions between oil and foam. These interactions are governed by three main mechanisms: entry of oil droplets into the gas–liquid interface, spreading of oil on the gas–liquid interface, and formation of an unstable bridge across lamellae [27–30]. These three mechanisms can be quantified as a function of the interfacial tensions between oil, gas, and water by evaluating the entering coefficient (E), spreading coefficient (S), and bridging coefficient (B) [26]. E, S, and B can be calculated as follows (Eqs. 3–5):

$$E = \sigma_{gw} + \sigma_{ow} - \sigma_{go} \tag{3}$$

$$S = \sigma_{gw} - \sigma_{ow} - \sigma_{go} \tag{4}$$

$$B = \sigma_{gw}^2 + \sigma_{ow}^2 - \sigma_{go}^2 \tag{5}$$

where σ_{gw}, σ_{ow}, and σ_{go} are the interfacal tensions between CO_2 and water, oil and water, and oil and CO_2, respectively. **Figure 4** presents a flowchart to predict the foam stability when in contact with oil, as indicated by the E, S, and B coefficients [27]. The oil droplets should be able to enter the gas-water interface to destabilize the foam. Once the entry condition is achieved (E is positive) and the oil droplets spread on the gas–liquid interface (S is positive), the gas/water interface will expand. As a result, the foam lamellae become thin and rupture, thus weakening the foam. If there is no spreading (S is negative) and the oil droplets form an emulsion at the gas/water interface, the foam film may rupture once oil droplets bridge between both surfaces of the lamellae (B is positive).

Ibrahim and Nasr-El-Din [23, 24] found that the AOS foam in contact with oil became unstable and decayed very fast, dissolving completely in 30 min compared

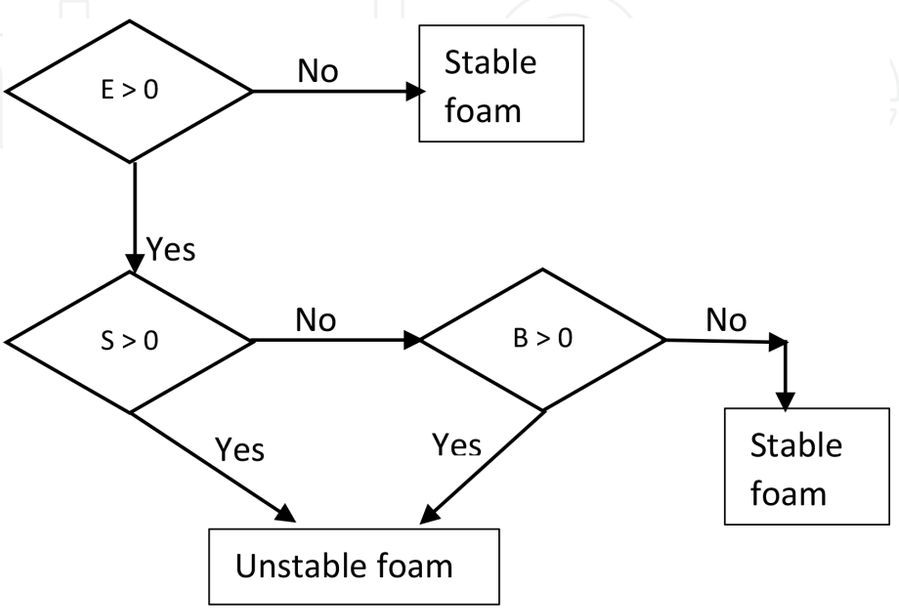

Figure 4.
Flowchart to predict foam stability from E, S, and B coefficients.

to more than 5 h in the absence of oil [24]. Two reasons account for the adverse effect of crude oil on foam decay. First, oil droplets tend to spread along with the gas/liquid interface. As a result, the stable gas/liquid interface becomes unstable, which accelerates the rupture of the foam lamellae. Second, oil forms an emulsion in the foam lamellae. The oil droplets in the unstable emulsion agglomerate and accelerate the drainage of the foam lamellae; hence, the foam decays faster [28].

In **Figure 3**, the crude oil forms layers in the interface between the gas and liquid phases, and an emulsion forms inside the AOS foam lamellas. **Figure 5** shows microscope images for AOS foam lamellae in the presence of oil. The oil droplets in the unstable emulsion agglomerate and accelerate the drainage, where the lamella thickness decreases over time. Hence, the foam becomes unstable and decay faster.

Figure 6 plots the foam height over time that gives indication for the decay rate from a visual cell experiment in which the foam lamellae were in contact with crude oil. At room temperature, the initial AOS foam height was 20 cm; then the foam decayed over time to reach 10 cm after 15 min (foam half-life = 15 min). In contact with oil, the foam decayed faster, and the half-life time decreased to 3 min.

Figure 7a shows the change of the normalized foam half-life as a function of temperature. The normalized half-life time is the half-life time for the foam system divided by the half-life time of AOS system at room temperature without crude oil. With increasing temperature, the foam became unstable and decayed more quickly than at room temperature. The half-life for the AOS system in the absence of crude oil at 150°F also decreased to 0.13 of its value at 77°F. As the temperature increases,

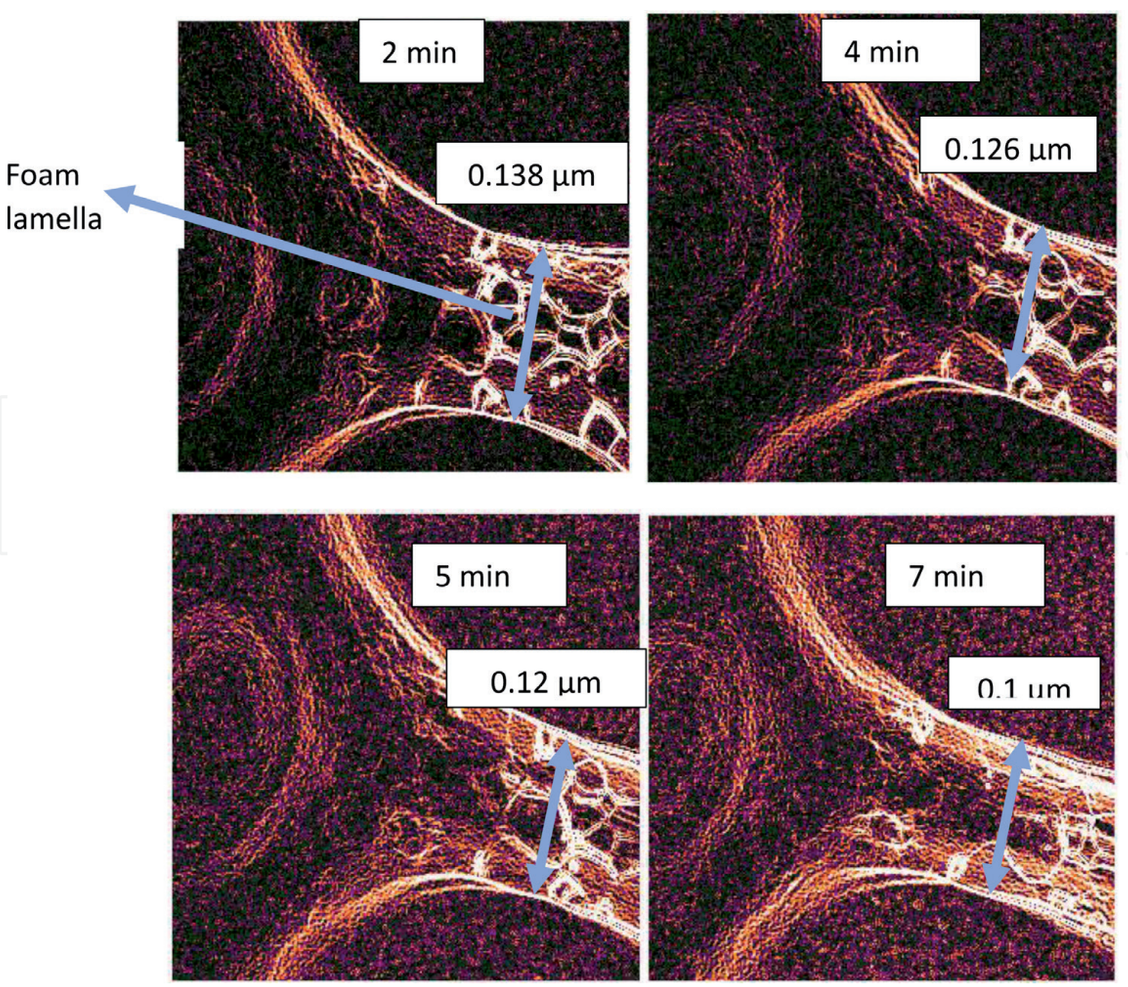

Figure 5.
Microscopic images for AOS foam to track the unstable emulsion and draining of the foam lamellae over time when in contact with the crude oil (20×) [23].

DOI: http://dx.doi.org/10.5772/intechopen.89301

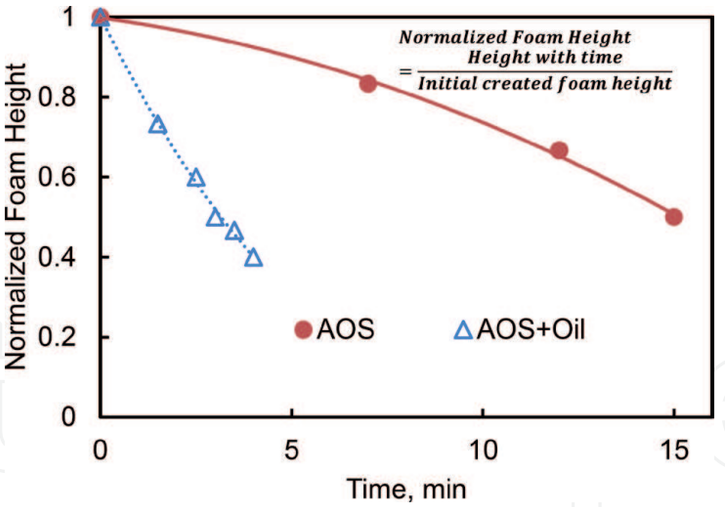

Figure 6.
Normalized foam height for AOS foam system in the absence and presence of crude oil as a function of time at 77°F and 800 psi.

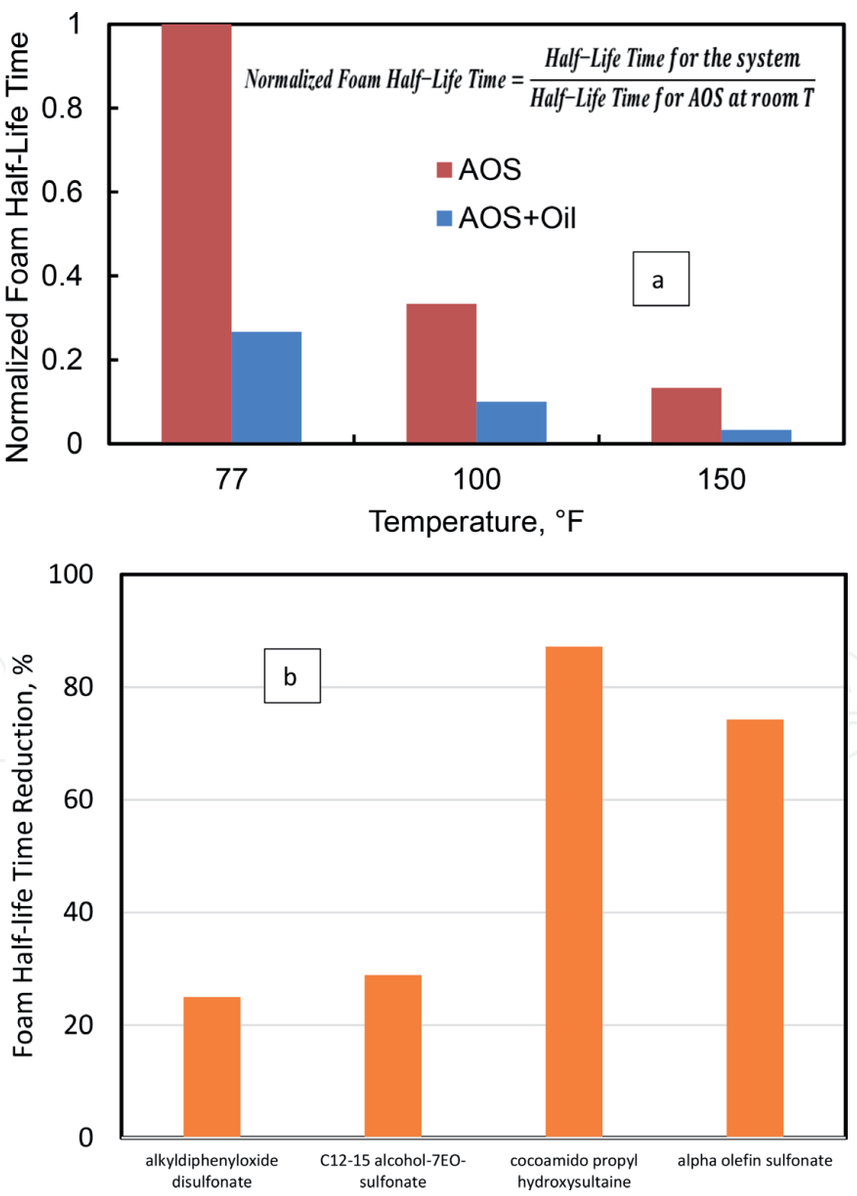

Figure 7.
Effect of 1 vol% crude oil in foam stability, (a) foam stability at different temperatures at 800 psi for 0.5 wt% AOS foam system and (b) foam half-life time reduction percent for different surfactant systems.

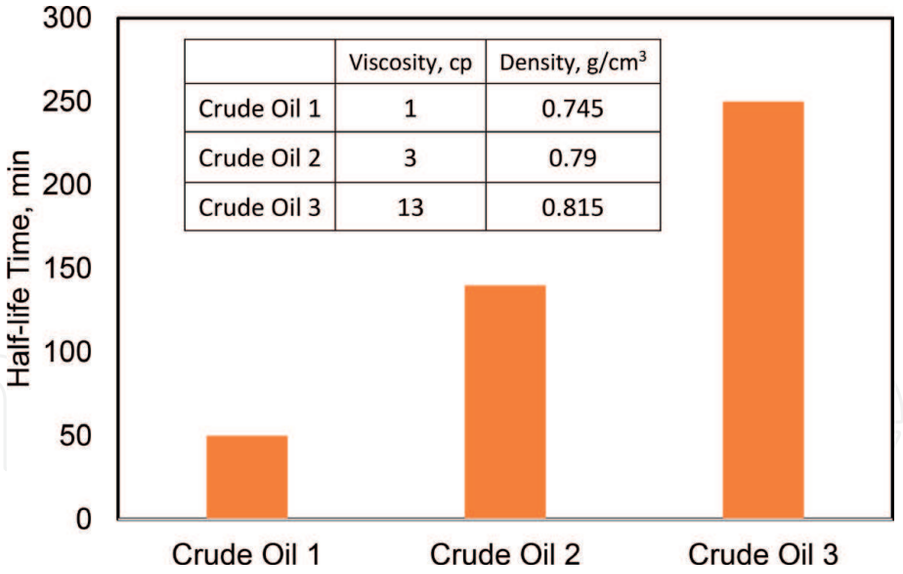

	Viscosity, cp	Density, g/cm^3
Crude Oil 1	1	0.745
Crude Oil 2	3	0.79
Crude Oil 3	13	0.815

Figure 8.
Effect of oil density and viscosity on foam stability [29].

the liquid viscosity decreases, which leads to faster drainage. As a result, gas bubbles coalesce faster [31]. In contact with crude oil, the AOS was not able to generate stable foam, where the half-life was 3.9 and 0.45 min at 77 and 150°F, respectively.

The E, S, and B coefficients for the AOS system at 150°F and 800 psi were found to be 7.96, 6.68 mN/m, and 231.74 $(mN/m)^2$. Based on the flowchart in **Figure 4**, the generated foam is not stable. Increasing the pressure to 1200 psi, the values for the three coefficients slightly decreased to 6.67, 5.38 mN/m, and 141.29 $(mN/m)^2$, still greater than zero. A positive E value indicates that the oil-entering condition was initially favorable. However, once the oil entered the foam system as an emulsion on the AOS and AOS/SiO_2 foam lamellae, it started to spread on the surfaces of the foam bubbles (S > 0) and generated unstable bridges (B > 0) that quickly broke the lamellae and destabilized the foam. The microscopic images of the AOS foam system in contact with crude oil in **Figures 3** and **5** confirm this behavior.

Similar results were observed by Simjoo et al. [27]. Adding 1 vol% crude oil to different surfactant systems decreases the foam stability and the half-life time. **Figure 7b** shows the change in the foam half-life time due to the presence of crude oil. Regardless of the surfactant type, adding crude oil to the foam increases the lamella drainage and decreases the foam stability.

The previous experimental results demonstrate the detrimental effect of crude oil on foam stability [29]. However, regardless of the surfactant used, crude oil with higher hydrocarbon chain lengths has a lower effect on foam stability. **Figure 8** shows the half-life of Coco/SDS (a foam system with a 1:1 mixture of cocobetaine and sodium dodecyl sulfate surfactants) in contact with different crude oils with different densities and viscosities at room temperature. These data show that the higher the density and viscosity, the lower the effect of crude oil on foam stability.

5. Improving foam stability using nanoparticles

The previous section shows the instability of foam systems in contact with crude oil at high temperature. Nanoparticles have been examined extensively as a means to stabilize foams used in oil-production operations, including those in high-salinity and high-temperature environments [9, 20–25, 32, 33]. This behavior is due to the nanoparticles' adsorption to the interface between the gas and liquid phases and minimizes the

DOI: http://dx.doi.org/10.5772/intechopen.89301

contact area between them; as a result, they can build a strong barrier that prevents bubble coalescence. **Figure 9a** shows a microscopic image for SDS foam system that was stabilized with Al_2O_3 nanoparticles [32]. It shows the nanoparticle adsorption at the lamella surface. Hence, the nanoparticle-stabilized foams are expected to be durable and highly resistant to unfavorable reservoir conditions including high salinity, high temperatures, and the presence of crude oil. Silica nanoparticles are currently regarded as most effective for improving foam stability [20–25].

Nanoparticles' size greatly affect the foam stability. Different experimental results for the usage of silica nanoparticles showed that the smaller the nanoparticle size, the higher the foam stability [32]. The small particle will move faster to the gas–liquid interface compared to the larger nanoparticle size. Hence, the nanoparticle adsorption and concentration in the lamella surface increase and the foam become more stable. This behavior of foam stability with nanoparticle size greatly depends on foam quality, salinity, and nanoparticle hydrophobicity. Larger-size nanoparticles improve the foam stability at foam quality of 70–80%, while smaller size nanoparticles improve the foam stability at quality of 50–60% [9]. In addition, 140 nm silica nanoparticles with contact angle of 86° increased the foam stability greater than 100 nm silica nanoparticles with contact angle of 54° [21].

Emrani et al. [21] studied the effect of adding 140 nm silica nanoparticles to AOS foam system. This work achieved a stable foam with an MRF of 8, which was four

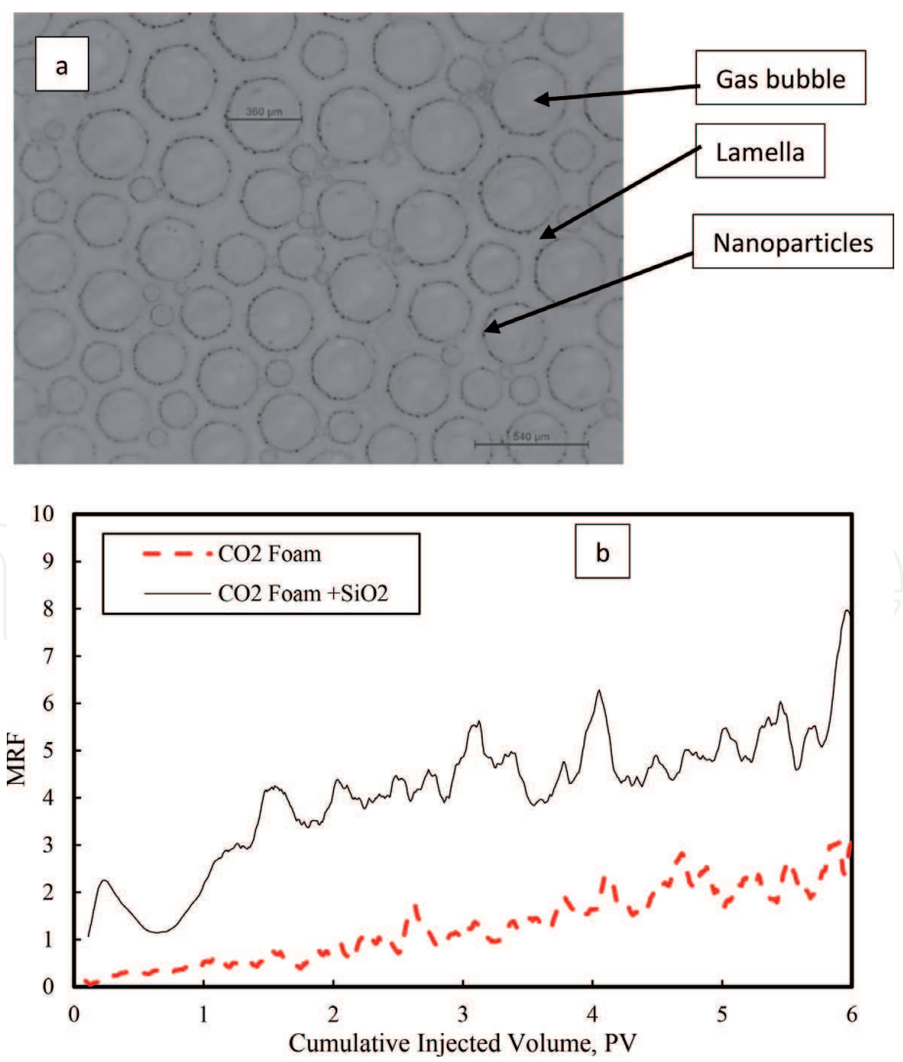

Figure 9.
Foam stability improvement by nanoparticles, (a) microscopic image for SDS/Al_2O_3 foam system [32] and (b) MRF for 0.5 wt% AOS solutions in the absence and presence of 0.1 wt% nanoparticles at 77°F [21].

times the MRF for AOS foam system. Adding nanoparticles creates a fine texture foam that increases the apparent viscosity and the MRF (**Figure 9b**). Similarly, in a bulk stability test, adding nanoparticles to the AOS foam system tripled the half-life of its original value without nanoparticles [24]. In addition, nanoparticles are adsorb on the interface between the gas and liquid phases, creating thick, solid films that provide a barrier to film thinning and inter-bubble diffusion. Hence, in the presence of crude oil, the spreading of the oil droplets along the foam lamellae decreases and prevents bridge formation. Interfacial tension (IFT) measurements for silica nanoparticle foam system showed that the spreading and bridging coefficients have negative values (−0.69, −4.43 at 1200 psi and 150°F), thus evidencing improved foam stability.

Nanoparticle concentration in the interface between the liquid and gas phases is a critical parameter and should increase to a certain threshold to stabilize the foam [34]. **Figure 10** shows the change in foam half-life time with increasing silica nanoparticle concentrations. At low concentrations, the liquid/gas interface is not saturated, and low foam stability is generated. With increased nanoparticle concentration, foam stability increases. However, at higher concentration, nanoparticles agglomerate and form bigger particles that negatively impact the foam stability. Zeta potential measurements in **Figure 10** show a reduction of the absolute zeta potential value with increasing nanoparticle concentration from 0.1 to 0.2 wt%, which indicates a stable suspension. At nanoparticles' concentration higher than 0.2 wt%, nanoparticles become unstable and agglomerate which is indicated by increasing the zeta potential value.

Coreflood experiments by Ibrahim and Nasr-El-Din [23, 24] compared EOR results using an AOS foam system versus a silica-nanoparticle system. **Figure 11** shows total oil recovery after tertiary recovery using different foam systems. A water-assisted gas (WAG) system was able to increase the oil recovery to 60%. AOS generated a weak foam with a similar MRF to that of the CO_2/water system, and oil recovery increased by 1.8%. Adding silica nanoparticles to the foam system increased oil recovery to 68.2%.

In a high-salinity environment, the absolute zeta potential for suspensions will decrease [35]. As a result, nanoparticles will have a high affinity to agglomerate. To prevent the instability of nanoparticles in a high-salinity environment, surface-modified nanoparticles were used to provide steric repulsion between particles.

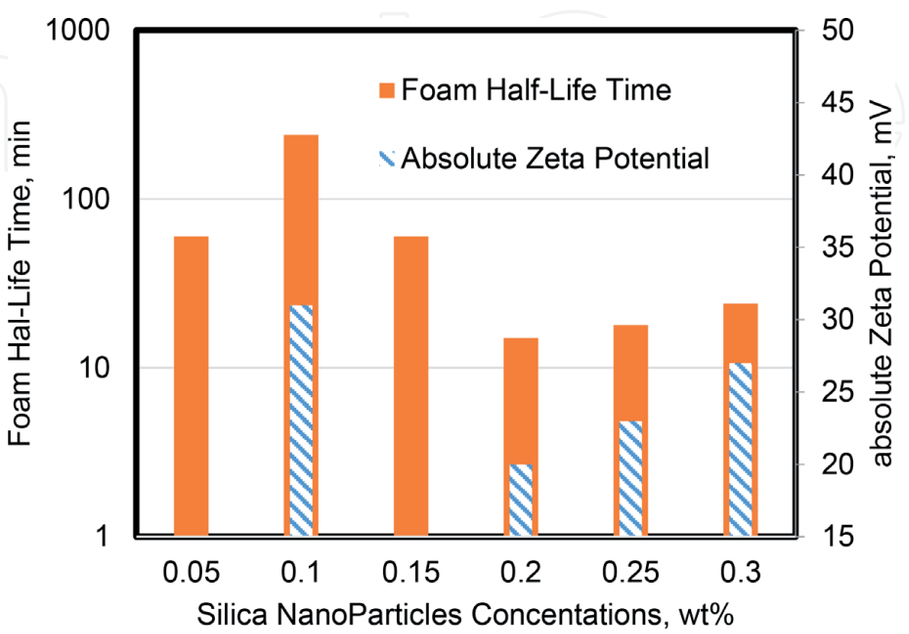

Figure 10.
Effect of silica nanoparticle concentrations on foam stability.

DOI: http://dx.doi.org/10.5772/intechopen.89301

Nanoparticle surface wettability is another critical parameter of foam stability. Generally, nanoparticle surfaces should be hydrophilic enough to disperse in water but hydrophobic enough to accumulate at the interface between the water and gas. Nanoparticles coated with 50% SiOH dichlorodimethylsilane generated a stable foam compared to polyethylene glycol (PEG)-coated nanoparticles or dichlorodimethylsilane-coated nanoparticles with higher SiOH% even at 8 wt% NaCl salt concentration [36].

In addition to silica, other types of nanoparticles can also be used to improve foam stability. About 0.1 wt% Fe_2O_3 nanoparticles were able to increase the AOS foam half-life time from 1 to 7 h at 75°F and 300 psi [37]. However, these nanoparticles tend to aggregate due to their large surface area, which is confirmed by low absolute zeta potential values. An experimental work by Bayat et al. [38] compared the foam stability using SiO_2, Al_2O_3, TiO_2, and CuO nanoparticles. They found that the optimum concentration for these nanoparticles was 0.008 wt%. **Figure 12** shows the recovery factor and foam half-life for the four different systems. SiO_2 foam had the highest foam stability and oil recovery compared to the other nanoparticles.

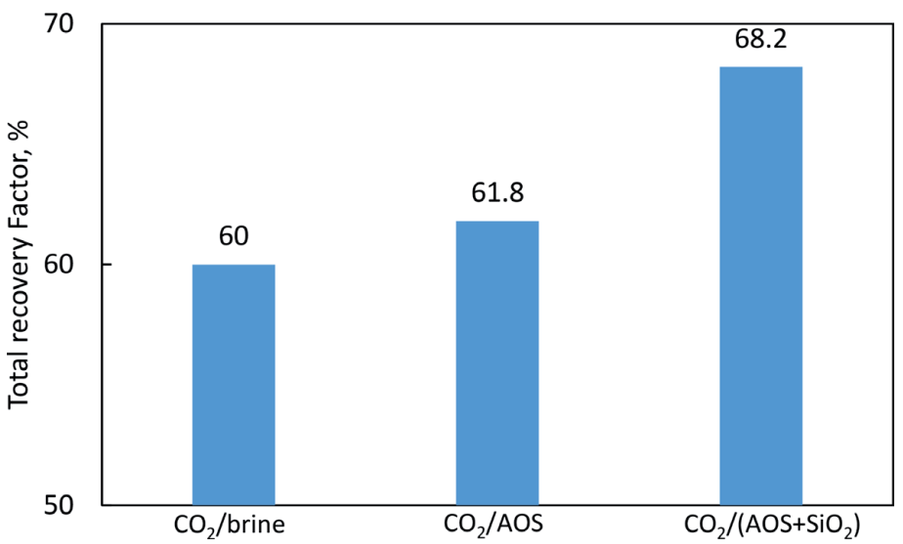

Figure 11.
Total oil recovery for different foam systems with adding 0.5 wt% AOS surfactant and 0.1 wt% silica nanoparticles.

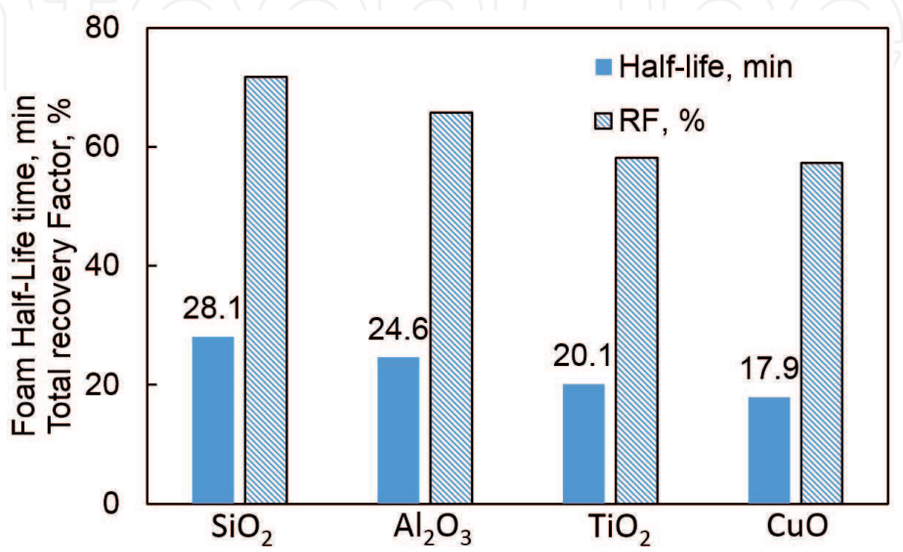

Figure 12.
Effect of nanoparticle type on the foam stability and oil recovery factor.

6. Improving foam stability using viscosifiers

The addition of thickeners such as polymers or viscoelastic surfactant (VES) to CO_2 foam improves foam stability by increasing lamella viscosity that delays

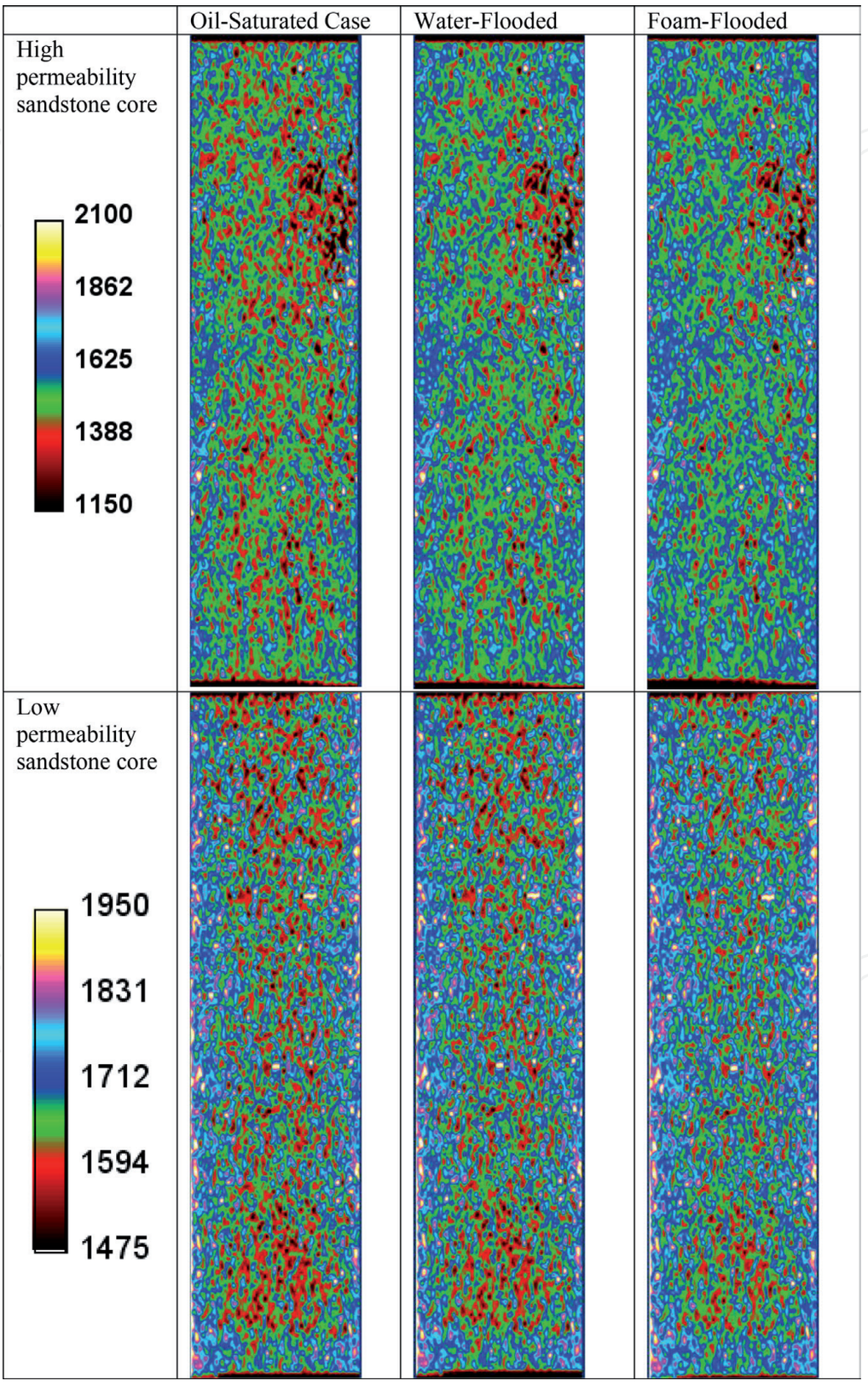

Figure 13.
CT scan scans for Boise and Berea cores during the dual-core flood experiment after oil saturation, waterflooding, and foam-flooding stages.

the lamella drainage effect at high temperature and in contact with crude oils [23, 33, 39, 40].

A dual coreflood experiment was conducted by Ibrahim and Nasr-El-Din [23, 24] to investigate the divergent ability of VES-stabilized foam in heterogeneous formations (with permeability contrast of 700/100). The VES was able to increase the foam stability and improve the sweep efficiency. The oil recovery after the waterflooding stage was 19 and 55% from the low and the high-permeability cores, respectively. Low sweep efficiency in the low-permeability cores was found where the residual oil saturation was 36 vol% compared to 31 vol% in the high-permeability core. When injecting VES into the foam system, the sweep efficiency improved, and the residual oil saturation decreased to 23 and 27 vol% in the low- and the high-permeability cores, respectively. The total oil recovery after foam injection was found to be 50 and 62 vol% of the original oil in place (OOIP).

Figure 13 shows oil saturation distribution along the two cores after the foam-flooding stage compared to the oil-saturated and the waterflooded cases. For the high-permeability core, most of the oil was produced during waterflooding, and the recovery factor increased only by 10% after foam flooding. The slight change in distribution of the red areas in **Figure 13** indicates oil recovery from the waterflooded and the foam-flooded cases. In the case of low-permeability core, most of the reduction in the red color distribution happened after foam flooding.

Figure 14 shows the results of using polymers as a thickener to improve the foam stability [41]. Wei et al. [41] used xanthan gum (molecular weight of 50–100 × 10^4) to improve the foam stability for a sulfobetaine-based surfactant foam system at 90°C and 1450 psi. As the polymer concentration increases, the liquid phase viscosity increases. As a result, lamella drainage decreases, and foam-stability half-life increases. However, an increase in polymer concentration also increases the surface-tension forces and thus decreases the system foamability. Stable foam with a higher half-life increases the apparent viscosity for the displacing fluid that improves the sweep efficiency. The oil recovery for the polymer-foam system was 43.2%, compared to 21.8% in the case of the polymer-free foam system.

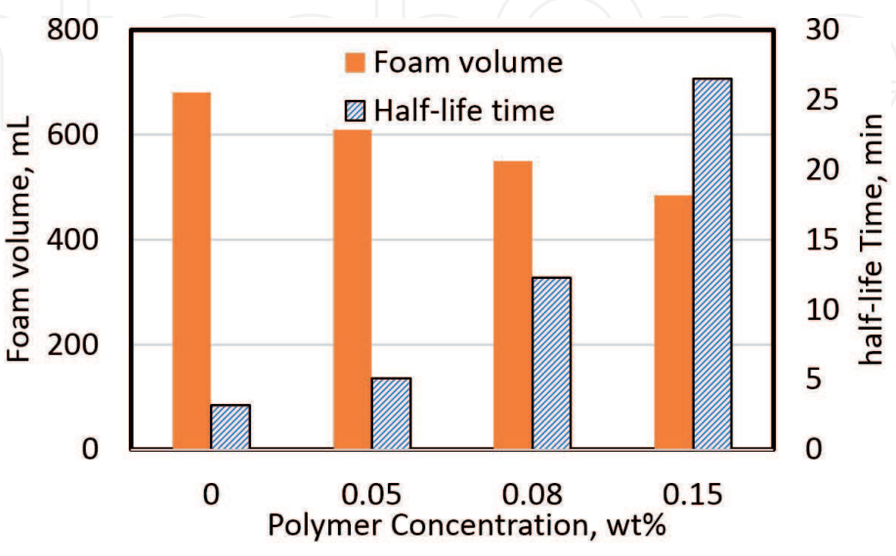

Figure 14.
Effect of polymer concentration on the generated foam volume and its half-life.

7. Summary

This chapter reviews the application of CO_2 foam in enhanced oil recovery and establishes the following main points:

1. Foam lamellae can be generated by a snap-off, lamella division, and leave-behind mechanisms. The foam generated by the leave-behind mechanism is weak because the lamellae are parallel to the flow direction.

2. Crude oil has a negative impact on foam stability, and its deterioration effect can be determined by calculating entering, spreading, and bridging coefficients as a function of oil/gas/water interfacial tension.

3. In harsh environments such as those with high salinity or high temperature, nanoparticles can be used to improve foam stability. SiO_2 with the modified surface was found to be the more effective and popular nanoparticles in foam-stability applications.

4. At high-temperature conditions, VES can be used as a thickener to decrease the rates of lamella drainage and foam decay.

CO_2 foam can be used to improve the oil recovery in EOR process. However, surfactant-based foam provides unstable, and low sweep efficiency will be observed. As a result, nanoparticles or viscosifiers should be used to improve the foam stability.

Acknowledgements

We thank Gia Alexander for proofreading the chapter.

Nomenclature

A	cross-section area of the core
AOS	alpha-olefin sulfonate
B	bridging coefficient
CMC	critical micelle concentration
CT	X-ray computed tomography
E	entering coefficient
EOR	enhanced oil recovery
K	absolute core permeability, md
k_e	effective fluid permeability, md
L	core length
M	mobility of the displacing fluid to the displaced fluid ratio
MRF	mobility reduction factor
PEG	polyethylene glycol
Q	total flow rate
S	spreading coefficient
Δp	pressure drop across the core
λ	fluid mobility, md/cp
μ	fluid viscosity, cp
σ_{gw}, σ_{ow}, and σ_{go}	interfacal tensions between CO_2 and water, oil and water, and oil and CO_2, respectively

DOI: http://dx.doi.org/10.5772/intechopen.89301

IntechOpen

Author details

Ahmed Farid Ibrahim* and Hisham A. Nasr-El-Din
Texas A&M University, College Station, TX, USA

*Address all correspondence to: ahmedmfaried@gmail.com

References

[1] Gozalpour F, Ren S, Tohidi B. CO_2 EOR and storage in oil reservoir. Oil & Gas Science and Technology. 2005;**60**(3):537-546

[2] Rezk MG, Foroozesh J, Zivar D, Mumtaz M. CO_2 storage potential during CO2 enhanced oil recovery in sandstone reservoirs. Journal of Natural Gas Science and Engineering. 2019;**66**:233-243

[3] Han J, Lee M, Lee W, Lee Y, Sung W. Effect of gravity segregation on CO_2 sequestration and oil production during CO_2 flooding. Applied Energy. 2016;**161**:85-91

[4] Chen Y, Elhag AS, Poon BM, Cui L, Ma K, Liao SY, et al. Ethoxylated cationic surfactants for CO2 EOR in high temperature, high salinity reservoirs. In: SPE Improved Oil Recovery Symposium; 2012/1/1. Tulsa, Oklahoma, USA: SPE: Society of Petroleum Engineers; 2012. p. 15

[5] Zhang Y, Huang SS, Luo P. Coupling immiscible CO_2 technology and polymer injection to maximize EOR performance for heavy oils. Journal of Canadian Petroleum Technology. 2010;**49**(05):25-33

[6] Dai C. Chapter seven—formation damage during chemical flooding. In: Yuan B, Wood DA, editors. Formation Damage During Improved Oil Recovery. Cambridge, MA: Gulf Professional Publishing; 2018. pp. 275-304

[7] Yuan B, Wood DA. A comprehensive review of formation damage during enhanced oil recovery. Journal of Petroleum Science and Engineering. 2018;**167**:287-299

[8] Bian Y, Penny GS, Sheppard NC. Surfactant formulation evaluation for carbon dioxide foam flooding in heterogeneous sandstone reservoir. In: SPE Improved Oil Recovery Symposium; 2012/1/1. Tulsa, Oklahoma, USA: SPE: Society of Petroleum Engineers; 2012. p. 16

[9] Xiao C, Balasubramanian SN, Clapp LW. Rheology of viscous CO_2 foams stabilized by nanoparticles under high pressure. Industrial & Engineering Chemistry Research. 2017;**56**(29):8340-8348

[10] Negin C, Ali S, Xie Q. Most common surfactants employed in chemical enhanced oil recovery. Petroleum. 2017;**3**(2):197-211

[11] Farajzadeh R, Krastev R, Zitha PLJ. Foam films stabilized with alpha olefin Sulfonate (AOS). Colloids and Surfaces A: Physicochemical and Engineering Aspects. 2008;**324**(1):35-40

[12] Schramm LL. Foams: Fundamentals and Applications in the Petroleum Industry. Washington, DC: American Chemical Society; 1994

[13] Belyadi H, Fathi E, Belyadi F. Chapter five - hydraulic fracturing fluid systems. In: Belyadi H, Fathi E, Belyadi F, editors. Hydraulic Fracturing in Unconventional Reservoirs. Boston: Gulf Professional Publishing; 2017. pp. 49-72

[14] Liu Y, Grigg RB, Bai B. Salinity, pH, and surfactant concentration effects on CO2-foam. In: SPE International Symposium on Oilfield Chemistry; 2005/1/1. The Woodlands, Texas: SPE: Society of Petroleum Engineers; 2005. p. 11

[15] Yin G, Grigg RB, Svec Y. Oil recovery and surfactant adsorption during CO2-foam flooding. In: Offshore Technology Conference; 2009/1/1. Houston, Texas: OTC: Offshore Technology Conference; 2009. p. 14

[16] Falls AH, Hirasaki GJ, Patzek TW, Gauglitz DA, Miller DD, Ratulowski T. Development of a mechanistic foam simulator: The population balance and generation by snap-off. SPE Reservoir Engineering. 1988;**3**(03):884-892

[17] Chen M, Yortsos YC, Rossen WR. Insights on foam generation in porous media from pore-network studies. Colloids and Surfaces A: Physicochemical and Engineering Aspects. 2005;**256**(2):181-189

[18] Emadi A, Sohrabi M, Jamiolahmady M, Irland S, Robertson G. Mechanistic study of improved heavy oil recovery by CO2-foam injection. In: SPE Enhanced Oil Recovery Conference; 2011/1/1. Kuala Lumpur, Malaysia: SPE: Society of Petroleum Engineers; 2011. p. 19

[19] Hematpur H, Mahmood SM, Nasr NH, Elraies KA. Foam flow in porous media: Concepts, models and challenges. Journal of Natural Gas Science and Engineering. 2018;**53**:163-180

[20] Ibrahim AF, Emrani A, Nasr-El-Din H. Stabilized CO_2 foam for EOR applications. In: Carbon Management Technology Conference; 2017/8/24. Houston, Texas, USA: CMTC: Carbon Management Technology Conference; 2017. p. 19

[21] Emrani AS, Ibrahim AF, Nasr-El-Din HA. Mobility control using nanoparticle-stabilized CO_2 foam as a hydraulic fracturing fluid. In: SPE Europec Featured at 79th EAGE Conference and Exhibition; 2017/6/12. Paris, France: SPE: Society of Petroleum Engineers; 2017. p. 16

[22] Singh R, Mohanty KK. Foam flow in a layered, heterogeneous porous medium: A visualization study. Fuel. 2017;**197**:58-69

[23] Farid Ibrahim A, Nasr-El-Din H. An experimental study for the using of nanoparticle/VES stabilized CO2 foam to improve the sweep efficiency in EOR applications. In: SPE Annual Technical Conference and Exhibition; 2018/9/24. Dallas, Texas, USA: SPE: Society of Petroleum Engineers; 2018. p. 15

[24] Farid Ibrahim A, Nasr-El-Din H. Stability improvement of CO2 foam for enhanced oil recovery applications using nanoparticles and viscoelastic surfactants. In: SPE Trinidad and Tobago Section Energy Resources Conference; 2018/6/22. Port of Spain, Trinidad and Tobago: SPE: Society of Petroleum Engineers; 2018. p. 17

[25] Khajehpour M, Etminan SR, Goldman J, Wassmuth F, Bryant S. Nanoparticles as foam stabilizer for steam-foam process. SPE Journal. 2018;**23**(06):2232-2242

[26] Lau HC, O'Brien SM. Effects of spreading and nonspreading oils on foam propagation through porous media. SPE Reservoir Engineering. 1988;**3**(03):983-986

[27] Simjoo M, Rezaei T, Andrianov A, Zitha PLJ. Foam stability in the presence of oil: Effect of surfactant concentration and oil type. Colloids and Surfaces A: Physicochemical and Engineering Aspects. 2013;**438**:148-158

[28] Koczo K, Lobo LA, Wasan DT. Effect of oil on foam stability: Aqueous foams stabilized by emulsions. Journal of Colloid and Interface Science. 1992;**150**(2):492-506

[29] Osei-Bonsu K, Shokri N, Grassia P. Foam stability in the presence and absence of hydrocarbons: From bubble- to bulk-scale. Colloids and Surfaces A: Physicochemical and Engineering Aspects. 2015;**481**:514-526

[30] Schramm LL, Novosad JJ. The destabilization of foams for improved

oil recovery by crude oils: Effect of the nature of the oil. Journal of Petroleum Science and Engineering. 1992;**7**(1):77-90

[31] Kapetas L, Vincent Bonnieu S, Danelis S, Rossen WR, Farajzadeh R, Eftekhari AA, et al. Effect of temperature on foam flow in porous media. Journal of Industrial and Engineering Chemistry. 2016;**36**:229-237

[32] Yekeen N, Manan MA, Idris AK, Padmanabhan E, Junin R, Samin AM, et al. A comprehensive review of experimental studies of nanoparticles-stabilized foam for enhanced oil recovery. Journal of Petroleum Science and Engineering. 2018;**164**:43-74

[33] Zhu J, Yang Z, Li X, Hou L, Xie S. Experimental study on the microscopic characteristics of foams stabilized by viscoelastic surfactant and nanoparticles. Colloids and Surfaces A: Physicochemical and Engineering Aspects. 2019;**572**:88-96

[34] Kim I, Taghavy A, DiCarlo D, Huh C. Aggregation of silica nanoparticles and its impact on particle mobility under high-salinity conditions. Journal of Petroleum Science and Engineering. 2015;**133**:376-383

[35] Ibrahim AF, Nasr-El-Din HA. Effect of water salinity on coal wettability during CO_2 sequestration in coal seams. Energy & Fuels. 2016;**30**(9):7532-7542

[36] Worthen AJ, Bagaria HG, Chen Y, Bryant SL, Huh C, Johnston KP. Nanoparticle-stabilized carbon dioxide-in-water foams with fine texture. Journal of Colloid and Interface Science. 2013;**391**:142-151

[37] Emrani AS, Nasr-El-Din HA. Stabilizing CO_2 foam by use of nanoparticles. SPE Journal. 2017;**22**(02):494-504

[38] Bayat AE, Rajaei K, Junin R. Assessing the effects of nanoparticle type and concentration on the stability of CO_2 foams and the performance in enhanced oil recovery. Colloids and Surfaces A: Physicochemical and Engineering Aspects. 2016;**511**:222-231

[39] Nasr-El-Din H, Chesson J, Cawiezel K, Devine C. Laboratory Investigation and Field Evaluation of Foamed VES Diversion Applied During Coiled-Tubing Matrix-Acid Treatment. paper SPE.99651:4-5

[40] Fang J, Dai C, Yan Y, Yan Z, You Q, editors. Enhanced foam stability by adding dispersed particle gel: A new 3-phase foam study. In: SPE Asia Pacific Enhanced Oil Recovery Conference. Society of Petroleum Engineers; 2015

[41] Wei P, Pu W, Sun L, Pu Y, Li D, Chen Y. Role of water-soluble polymer on foam-injection process for enhancing oil recovery. Journal of Industrial and Engineering Chemistry. 2018;**65**(01):280-289